Chapter 3

The Hodgkin–Huxley model of the action potential

This chapter presents the first quantitative model of active membrane properties, the **Hodgkin–Huxley model**. This was used to calculate the form of the action potentials in the squid giant axon. Our step-by-step account of the construction of the model shows how Hodgkin and Huxley used the **voltage clamp** to produce the experimental data required to construct mathematical descriptions of how the sodium, potassium and leak currents depend on the membrane potential. Simulations of the model produce action potentials similar to experimentally recorded ones and account for the threshold and refractory effects observed experimentally. While subsequent experiments have uncovered limitations in the Hodgkin–Huxley model descriptions of the currents carried by different ions, the **Hodgkin–Huxley formalism** is a useful and popular technique for modelling channel types.

3.1 The action potential

In the previous chapter we described the basis of the membrane resting potential and the propagation of signals down a passive neurite. We now explain a widespread feature of signalling in the nervous system: the **action potential**.

Intracellular recordings (Figure 3.1) demonstrate that action potentials are characterised by a sharp increase in the membrane potential (**depolarisation** of the membrane) followed by a somewhat less sharp decrease towards the resting potential (**repolarisation**). This may be followed by an afterhyperpolarisation phase in which the membrane potential falls below the resting potential before recovering gradually to the resting potential. The main difference between the propagation of action potentials and passive propagation of signals is that action potentials are **regenerative**, so their magnitude does not decay during propagation.

Hodgkin and Huxley (partly in collaboration with Katz) were the first to describe the active mechanisms quantitatively (Hodgkin *et al.*, 1952; Hodgkin and Huxley, 1952a, b, c, d). Their work proceeded in three main stages:

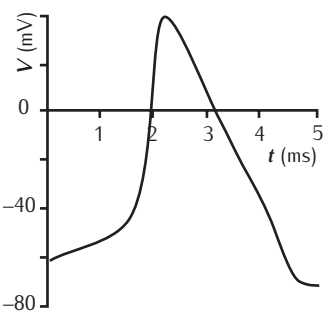

Fig. 3.1 The squid giant axon action potential. Simulated action potential in the squid giant axon at 6.3 °C.

(1) They recorded intracellularly from the squid giant axon. They used a voltage clamp amplifier in space clamp configuration (Box 3.1) to look at how current flow depends on voltage. By changing the extracellular concentration of sodium, they were able to infer how much of the current was carried by sodium ions and how much by other ions, principally potassium.

(2) They fitted these results to a mathematical model. Part of the model is the theoretically motivated framework developed in Chapter 2. Another part is based on the idea of ion-selective voltage-dependent gates controlled by multiple gating particles. The remainder of the model is determined by fitting curves to experimental data. The model is expressed in terms of a set of equations which are collectively called the **Hodgkin–Huxley model**, or **HH model** for short.

(3) They solved the equations defining the model to describe the behaviour of the membrane potential under various conditions. This involved solving the equations numerically. The simulated action potentials were very similar to the recorded ones. The threshold, propagation speed and refractory properties of the simulated action potentials also matched those of the recorded action potentials.

Their work earned them a Nobel prize in 1963, shared with Eccles for his work on synaptic transmission.

Hodgkin and Huxley were not able to deduce the molecular mechanisms underlying the active properties of the membrane, which was what they had set out to do (Box 3.3). Nevertheless, their ideas were the starting point for the biophysical understanding of the structures now known as ion channels, the basics of which are outlined in Chapter 5. Hille (2001) provides a comprehensive treatment of the structure and function of ion channels.

The HH model characterises two types of active channel present in the squid giant axon, namely a sodium channel and a potassium channel belonging to the family of potassium delayed rectifier channels. Work since 1952 in preparations from many different species has uncovered a large number of other types of active channel. Despite the age and limited scope of the HH model, a whole chapter of this book is devoted to it as a good deal of Hodgkin and Huxley's methodology is still used today:

(1) Voltage clamp experiments are carried out to determine the kinetics of a particular type of channel, though now the methods of recording and isolating currents flowing through particular channel types are more advanced.

(2) A model of a channel type is constructed by fitting equations, often of the same mathematical form, to the recordings. Modern methods of fitting equation parameters to data are covered later on, in Section 4.5.

(3) Models of axons, dendrites or entire neurons are constructed by incorporating models of individual channel types in the compartmental models introduced in Chapter 2. Once the equations for the models are solved, albeit using fast computers rather than by hand, action potentials and other behaviours of the membrane potential can be simulated.

Box 3.1 The voltage clamp

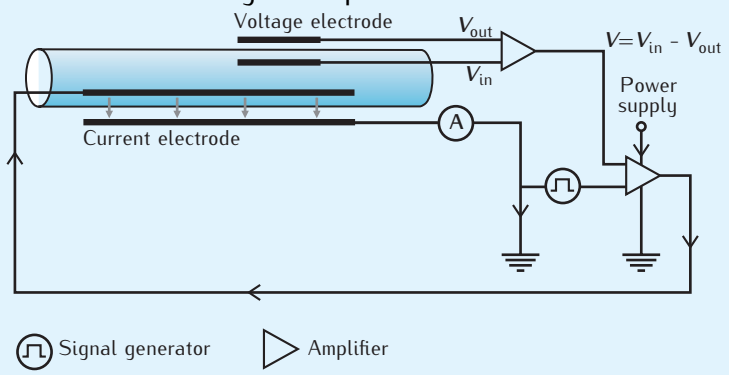

The next great experimental advance after intracellular recording was the voltage clamp. This was developed by Cole and Marmont in the 1940s at the University of Chicago (Marmont, 1949; Cole, 1968). Hodgkin, who was already working on a similar idea, learnt about the technique from Cole in 1947. The basic idea is to clamp the membrane potential to a steady value or to a time-varying profile, determined by the experimenter (see figure above). As with a current clamp (Chapter 2), an electrode is used to inject current I_e into the cell. At the same time, a voltage electrode records the membrane potential. The apparatus adjusts the injected current continually so that it is just enough to counteract deviations of the recorded membrane potential from the desired voltage value. This ensures that the membrane potential remains at the desired steady value or follows the required time-varying profile.

Hodgkin and Huxley used a **space clamp** configuration, where the electrodes are long, thin wires that short circuit the electrical resistance of the cytoplasm and the extracellular space. This ensures that the potential is uniform over a large region of membrane and that therefore there is no axial current in the region. There is no contribution to the membrane current from the axial current. In this configuration, the membrane current is identical to the electrode current, so the membrane current can be measured exactly as the amount of electrode current to be supplied to keep the membrane at the desired value.

To understand the utility of the voltage clamp, we recall that the membrane current I comprises a capacitive and an ionic current (Equation 3.1). When the voltage clamp is used to set the membrane potential to a constant value, no capacitive current flows as the rate of change in membrane potential, $\mathrm{d}V/\mathrm{d}t$, is zero. The voltage clamp current is then equal to the ionic current. Therefore, measuring the voltage clamp current means that the ionic current is being measured directly.

In this chapter, we focus on the second (modelling) and third (simulation) parts of the procedure. In Section 3.2, we begin with a step-by-step description of how Hodgkin and Huxley used a mixture of physical intuition and curve-fitting to produce their mathematical model. In Section 3.3, we look

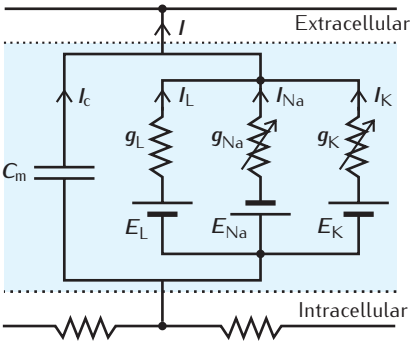

Fig. 3.2 The Hodgkin–Huxley equivalent electrical circuit.

at simulations of nerve action potentials using the model, and compare these with the experimental recordings. In Section 3.4 we consider how Hodgkin and Huxley corrected for temperature. Finally, in Section 3.5, we consider the simplifications inherent in the HH model and how to use the Hodgkin–Huxley formalism to build models of ion channels.

3.2 The development of the model

The starting point of the HH model is the equivalent electrical circuit of a compartment shown in Figure 3.2. There are three types of ionic current in the circuit: a **sodium current**, I_{Na}, a **potassium current**, I_K, and a current that Hodgkin and Huxley dubbed the **leak current**, I_L, which is mostly made up of chloride ions. The key difference between this circuit and the one presented in Chapter 2 is that the sodium and potassium conductances depend on voltage, as indicated by the arrow through their resistors. Since their properties change with the voltage across them, they are **active** rather than **passive** elements.

The equation that corresponds to the equivalent electrical circuit is:

$$I = I_c + I_i = C_m \frac{dV}{dt} + I_i, \tag{3.1}$$

where the **membrane current** I and the **capacitive current** I_c are as defined in Chapter 2. The total **ionic current** I_i is the sum of sodium, potassium and leak currents:

$$I_i = I_{Na} + I_K + I_L. \tag{3.2}$$

As defined in Section 2.4.1, the **driving force** of an ion is the difference between the membrane potential and the equilibrium potential of that ion. Hence, the sodium driving force is $V - E_{Na}$.

The magnitude of each type of ionic current is calculated from the product of the ion's driving force and the membrane conductance for that ion:

$$I_{Na} = g_{Na}(V - E_{Na}), \tag{3.3}$$

$$I_K = g_K(V - E_K), \tag{3.4}$$

$$I_L = \overline{g}_L(V - E_L), \tag{3.5}$$

where the sodium, potassium and leak conductances are g_{Na}, g_K and $\overline{g}_L$ respectively, and E_{Na}, E_K and E_L are the corresponding equilibrium potentials. The bar on the leakage conductance $\overline{g}_L$ indicates that it is a constant, in contrast with the sodium and potassium conductances which depend on the recent history of the membrane potential.

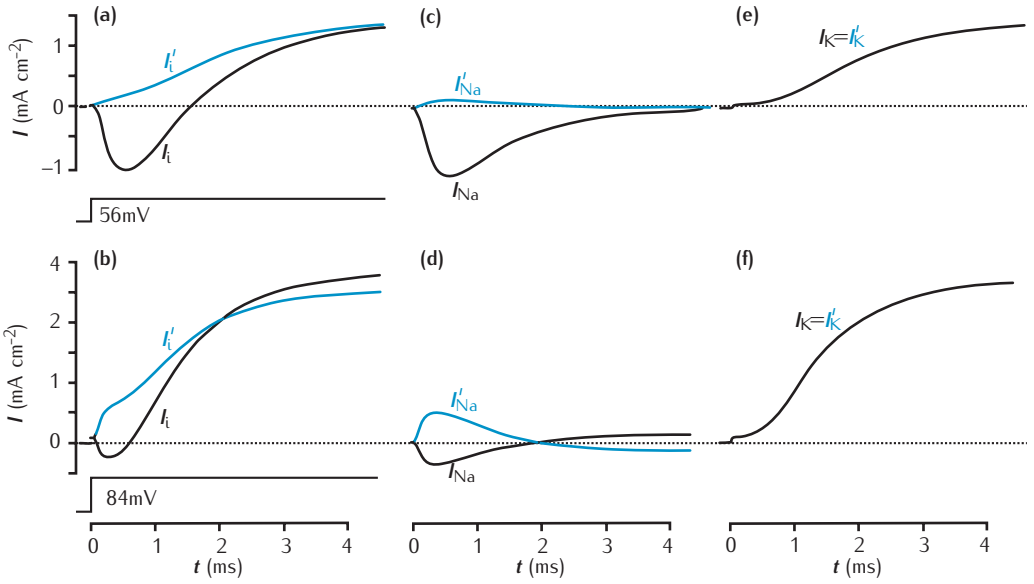

Fig. 3.3 The sodium current separated from the other currents using the ion substitution method (Box 3.2). **(a)** The ionic current in sea water (I_i) and in choline water (I'_i) in response to a voltage clamp of 56 mV (sea water) or 60 mV (choline water) above resting potential. **(b)** The same traces as **(a)**, but in response to a voltage clamp of 84 mV (sea water) and 88 mV (choline water) above resting potential. **(c,d)** The sodium currents in sea water (I_{Na}) and in choline water (I'_{Na}) inferred from pairs of ionic currents in **(a)** and **(b)**. **(e,f)** The potassium current in sea water (I_K) and in choline water (I'_K) inferred from the pairs of ionic currents in **(a)** and **(b)**, as described in the text. These two currents are, in fact, identical. The recording temperature was 8.5 °C. Adapted from Hodgkin and Huxley (1952a), with permission from John Wiley & Sons Ltd.

3.2.1 The potassium current

Hodgkin and Huxley measured the potassium conductance for a number of voltage clamp holding potentials. After first isolating the potassium current (Box 3.2 and Figure 3.3), they calculated the conductance using Equation 3.4. The form of the curves at each holding potential is similar to the example of the response to a holding potential of 25 mV above rest, shown in Figure 3.4a. Upon depolarisation, the conductance rises to a constant value. This rise in conductance is referred to as **activation**. The conductance stays at this peak value until the voltage is stepped back down to rest, where the conductance then decays exponentially (Figure 3.4b). The fall in conductance is called **deactivation**.

Box 3.2 The ion substitution method

In order to fit the parameters of their model, Hodgkin and Huxley needed to isolate the current carried by each type of ion. To do this they used the **ion substitution method**. They lowered the extracellular sodium concentration by replacing a proportion of the sodium ions in the standard extracellular solution (sea water) with impermeant choline ions. The currents recorded under voltage clamp conditions in sea water and in choline water were carried by sodium ions, potassium ions and other ions. On the assumption that the independence principle holds (Box 2.4), the currents carried by sodium ions in sea water and choline water differ, but the other ionic flows will remain the same. Therefore, the difference between currents recorded in sodium water and choline water can be used to infer the sodium current (Figure 3.3). Having isolated the sodium current and calculated the leak current by other methods, the potassium current can be deduced by subtracting the sodium and leak currents from the total current.

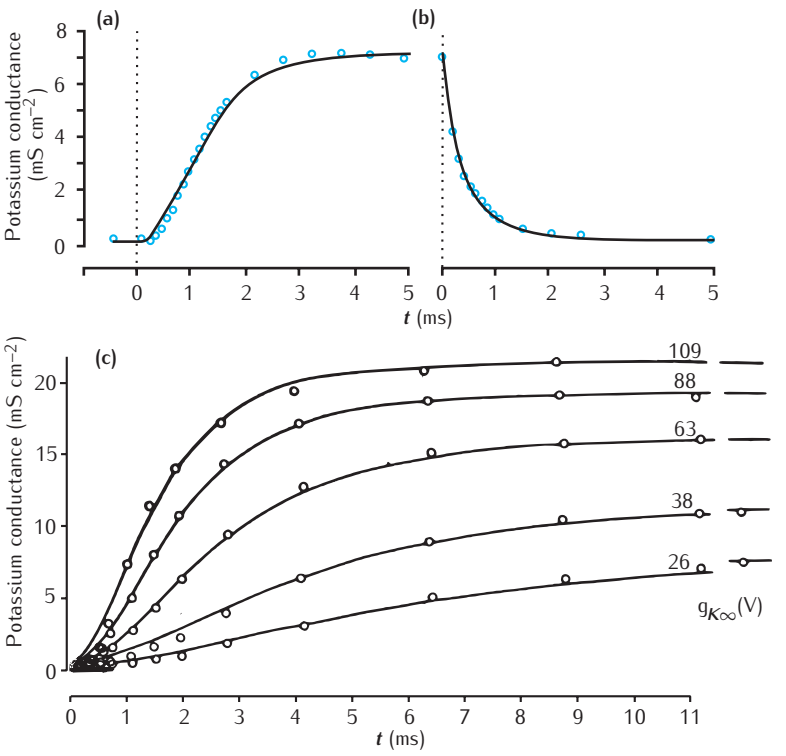

Fig. 3.4 Time course of the potassium conductance in a voltage clamp with **(a)** a step from resting potential to 25 mV above resting potential and **(b)** return to resting potential. The open circles represent data points derived from experiment. The solid lines are fits to the data (see text). **(c)** Time course of potassium conductance in response to voltage clamp steps to varying holding potentials; the voltage of the holding potential relative to rest is shown on each curve. Note that the activation of the conductance in response to a holding potential of 26 mV is slower than the activation in response to almost the same holding potential in **(a)**. This is due to a difference in recording temperatures: 21 °C in **(a)** and **(b)**, compared to 6 °C in **(c)**. Adapted from Hodgkin and Huxley (1952d), with permission from John Wiley & Sons Ltd.

The family of conductance activation curves (Figure 3.4c) show that there are two features of the curve that depend on the level of the voltage clamp holding potential:

(1) The value that the conductance reaches over time, $g_{K\infty}$, increases as the holding potential is increased. It approaches a maximum at high holding potentials. This implied that there was a **maximum potassium conductance** per unit area of membrane, which Hodgkin and Huxley denoted $\overline{g}_K$ and were able to estimate.

(2) The speed at which the limiting conductance is approached becomes faster at higher depolarising holding potentials.

The conductance curves show that the limiting conductance and the rate at which this limit is approached depends on the membrane voltage. Hodgkin and Huxley considered a number of models for describing this voltage dependence (Box 3.3). They settled on the idea of the membrane containing a number of **gates** which can be either closed to the passage of all ions or open to the passage of potassium ions. Each gate is controlled by a number of independent **gating particles**, each of which can be in either an open or closed position. For potassium ions to flow through a gate, *all* of the gating particles in the gate have to be in the open position.

The movement of gating particles between their closed and open positions is controlled by the membrane potential. The **gating variable** n is the probability of a single potassium gating particle being in the open state. As the gating particles are assumed to act independently of each other, the probability of the entire gate being open is equal to n^x, where x is the number

Box 3.3 Gating particles

Hodgkin and Huxley's goal had been to deduce the molecular mechanisms underlying the permeability changes evident in their experimental data. Reflecting on this later, Hodgkin (1976) wrote:

> although we had obtained much new information the overall conclusion was basically a disappointment .... As soon as we began to think about molecular mechanisms it became clear that the electrical data would by itself yield only very general information about the class of system likely to be involved. So we settled for the more pedestrian aim of finding a simple set of mathematical equations which might plausibly represent the movement of electrically charged gating particles.

Their initial hypothesis was that sodium ions were carried across the membrane by negatively charged carrier particles or dipoles. At rest these would be held by electrostatic forces. Consequently, they would not carry sodium ions in this state and, on depolarisation, they could carry sodium into the membrane. However, Hodgkin and Huxley's data pointed to a voltage-dependent gate. They settled on deriving a set of equations that would represent the theoretical movement of charged gating particles acting independently in a voltage-dependent manner.

In the contemporary view, the idea of gating particles can be taken to imply the notion of gated channels, but the hypothesis of ion pores or channels was not established at that time. Thus, though Hodgkin and Huxley proposed charged gating particles, it is perhaps tenuous to suggest that they predicted the structure of gated channels. Nevertheless, there is a correspondence between the choice of the fourth power for potassium conductance and the four subunits of the tetrameric potassium channel (Section 5.1).

of gating particles in the gate. Although, as described in Chapter 5, gating particles do not act independently, this assumption serves reasonably well in the case of potassium conductance in the squid giant axon. When there are large numbers of particles present, the large numbers ensure the proportion of particles being in the open position is very close to the probability n of an individual channel being in the open position, and the expected proportion of gates open is also the same as the probability of an individual gate being open, n^x.

The conductance of the membrane is given by the maximum conductance multiplied by the probability of a gate being open. For example, if each gate is controlled by four gating particles, as Hodgkin and Huxley's experiments suggested, the relationship between the potassium conductance g_K and gating particle open probability n is:

$$g_K = \overline{g}_K n^4. \tag{3.6}$$

If each potassium gate were dependent solely on a single theoretical gating particle, the conductance would be $\overline{g}_K n$.

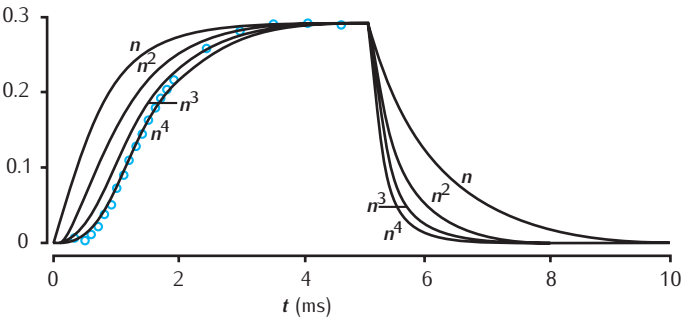

Fig. 3.5 A family of curves showing the time course of n raised to various powers. From top to bottom curves with n raised to the power 1, 2, 3 and 4 are shown. The parameters are as in Figure 3.4: $\tau_n(V_0) = 1.1$ ms, $\tau_n(V_1) = 0.75$ ms, $g_{K\infty}(V_0) = 0.09\,\text{mS cm}^{-2}$ and $g_{K\infty}(V_1) = 7.06\,\text{mS cm}^{-2}$. To compare the curves, the time course of n raised to the powers 2, 3 and 4 have initial and final values of n given by $(g_{K\infty}/\bar{g}_K)^{1/2}$, $(g_{K\infty}/\bar{g}_K)^{1/3}$, and $(g_{K\infty}/\bar{g}_K)^{1/4}$. The circular data points shown are the same as in Figure 3.4. Adapted from Hodgkin and Huxley (1952d), with permission from John Wiley & Sons Ltd.

The movement of a gating particle between its closed (C) and open (O) positions can be expressed as a reversible chemical reaction:

$$\mathrm{C} \underset{\beta_n}{\overset{\alpha_n}{\rightleftharpoons}} \mathrm{O}. \tag{3.7}$$

The fraction of gating particles that are in the O state is n, and the fraction in the C state is $1-n$. The variables α_n and β_n are **rate coefficients** which depend on the membrane potential; sometimes they are written $\alpha_n(V)$ and $\beta_n(V)$ to highlight their dependence on voltage. Just as rate laws govern the evolution of concentrations in chemical reactions, there is a **rate law** or **first order kinetic equation** corresponding to Equation 3.7, which specifies how the gating variable n changes over time:

$$\frac{\mathrm{d}n}{\mathrm{d}t} = \alpha_n(1-n) - \beta_n n. \tag{3.8}$$

The time course of the response of the gating variable n to a step change in membrane potential to a particular voltage V_1 can be determined by integrating Equation 3.8. A solution for the response of n to a voltage step is shown in Figure 3.5, along with the time courses of n raised to various powers. The curve for n looks roughly like the conductance curve shown in Figure 3.4. The main difference is that the theoretical time course of n is not S-shaped like the experimental curve; it has no initial inflection. As Figure 3.5 shows, when the time course of n in response to a positive voltage step is squared, cubed or raised to the power four, the resulting rising curve does have an inflection. The decaying part of the curve retains its decaying exponential shape. Hodgkin and Huxley found that raising n to the power four could give a better fit than cubing or squaring, suggesting that each gate contains four gating particles.

The general form of the time course for $n(t)$ in response to a voltage step is:

$$n(t) = n_\infty(V_1) - (n_\infty(V_1) - n_0)\exp(-t/\tau_n(V_1)), \tag{3.9}$$

where n_0 is the value of n at the start of the step, defined to be at time zero; the variables $n_\infty(V)$ and $\tau_n(V)$ are related to the rate coefficients $\alpha_n(V)$ and $\beta_n(V)$ by:

$$n_\infty = \frac{\alpha_n}{\alpha_n + \beta_n} \quad \text{and} \quad \tau_n = \frac{1}{\alpha_n + \beta_n}, \tag{3.10}$$

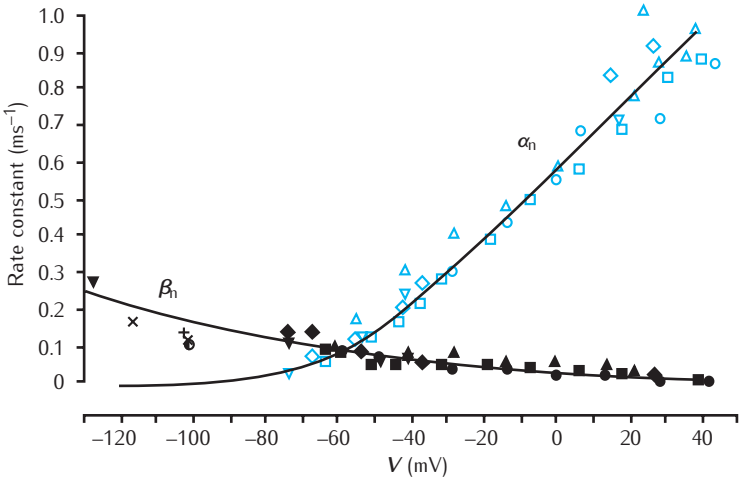

Fig. 3.6 Potassium rate coefficients α_n and β_n as a function of membrane potential. Blue symbols refer to measurements of α_n and black symbols to β_n. The shapes of the symbols identify the axon in which the value was recorded. Adapted from Hodgkin and Huxley (1952d), with permission from John Wiley & Sons Ltd.

where n_∞ is the limiting probability of a gating particle being open if the membrane potential is steady as t approaches infinity and τ_n is a time constant. When the membrane potential is clamped to V_1, the rate coefficients will immediately move to new values $\alpha_n(V_1)$ and $\beta_n(V_1)$. This means that, with the membrane potential set at V_1, over time n will approach the limiting value $n_\infty(V_1)$ at a rate determined by $\tau_n(V_1)$. The variables n_∞ and τ_n allow Equation 3.8 to be rewritten as:

$$\frac{dn}{dt} = \frac{n_\infty - n}{\tau_n}. \tag{3.11}$$

The final step in modelling the potassium current is to determine how the rate coefficients α_n and β_n in the kinetic equation of n (Equation 3.8) depend on the membrane potential. In using experimental data to determine these parameters, it is convenient to use the alternative quantities n_∞ and τ_n (Equation 3.10). The value of n_∞ at a specific voltage V may be determined experimentally by recording the maximum conductance attained at that voltage step, called $g_{K\infty}(V)$. Using Equation 3.6, the value of n_∞ at voltage V is then given by:

$$n_\infty(V) = \left(\frac{g_{K\infty}(V)}{\bar{g}_K}\right)^{\frac{1}{4}}. \tag{3.12}$$

The value for τ_n at a particular membrane potential is obtained by adjusting it so as to give the best match predicted time course of n given in Equation 3.9 and the data (Figure 3.4).

This process provides values for n_∞ and τ_n at various voltages. Hodgkin and Huxley converted them to the values for α_n and β_n using the inverse formulae to Equation 3.10:

$$\alpha_n = \frac{n_\infty}{\tau_n} \quad \text{and} \quad \beta_n = \frac{1 - n_\infty}{\tau_n}. \tag{3.13}$$

These experimental data points are shown in Figure 3.6, along with plots of the final fitted functions for α_n and β_n; see also Figure 3.10 for the equivalent

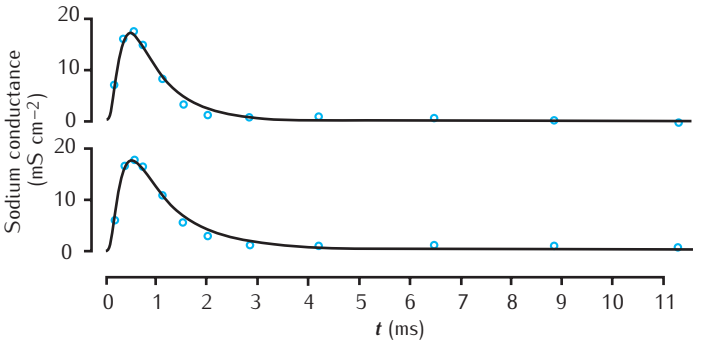

Fig. 3.7 Time course of the sodium conductance in a voltage clamp with a step change in voltage from resting potential to 76 mV and 88 mV above resting potential. The open circles represent data points derived from experiment. The solid lines are fits to the data (see text). Adapted from Hodgkin and Huxley (1952d), with permission from John Wiley & Sons Ltd.

n_∞ and τ_n plots. The equations for the functions $\alpha_n(V)$ and $\beta_n(V)$ are given in the summary of the entire set of equations describing the potassium ionic current through the membrane:

$$\begin{aligned} I_K &= \overline{g}_K n^4 (V - E_K), \\ \frac{dn}{dt} &= \alpha_n (1-n) - \beta_n n, \\ \alpha_n &= 0.01 \frac{V+55}{1-\exp(-(V+55)/10)}, \\ \beta_n &= 0.125 \exp(-(V+65)/80). \end{aligned} \tag{3.14}$$

3.2.2 The sodium ionic current

In a similar manner to the procedure used for potassium conductance, Hodgkin and Huxley isolated the sodium current and calculated the sodium conductance curves over a range of voltage clamp steps. The time course of the sodium conductance is illustrated in Figure 3.7. The most notable difference from the potassium conductance is that the sodium conductance reaches a peak and then decays back to rest, even while the clamped voltage remains in a sustained depolarising step. This reduction in conductance is termed **inactivation**, in contrast to deactivation (Section 3.2.1) when the reduction in conductance is due to termination of a voltage step. The time course of the conductance during inactivation differs from the time course during deactivation, and this suggested that two distinct processes can act to reduce the conductance.

The inactivation of the sodium conductance meant that Hodgkin and Huxley could not use the description they used for potassium, where there was just one gating variable, n. In order to quantify the inactivation process, Hodgkin and Huxley applied a range of voltage clamp experiments and protocols (Box 3.4 and Figures 3.8 and 3.9). They introduced a gating type variable, called h, to represent the level of inactivation. It could either be in the state of 'not inactivated' or the state of 'inactivated'. The rate of transition between these states is voltage dependent and governed by a first order kinetic equation similar to n:

$$\frac{dh}{dt} = \alpha_h (1-h) - \beta_h h. \tag{3.15}$$

As with the n gating particle, the voltage-dependent rate coefficients α_h and β_h can be reexpressed in terms of a limiting value h_∞ and a time constant τ_h. Hodgkin and Huxley's experiments suggested that sodium conductance was proportional to the inactivation variable h.

Hodgkin and Huxley completed their model of sodium conductance by introducing another gating particle which, like n, may be viewed as the proportion of theoretical gating particles that are in an open state, determining sodium conductance activation. They called this sodium activation particle m. As with n and h, the time course of m was governed by a first order kinetic equation with voltage-dependent forward and backward rates α_m and β_m:

$$\frac{dm}{dt} = \alpha_m(1-m) - \beta_m m. \tag{3.16}$$

As with potassium (Figure 3.5), the activation curve of the sodium conductance is inflected. The inflection was modelled satisfactorily by using three independent m gating particles, making the sodium conductance:

$$g_{Na} = \overline{g}_{Na} m^3 h. \tag{3.17}$$

This enabled a good fit to be made to experimental recordings by adjusting m_∞ and τ_m for different holding potentials and $\overline{g}_{Na}$ for all holding potentials. As with the gating variable n, Hodgkin and Huxley converted the limiting values and time constants of the m and h variables into rate coefficients (α_m, β_m and α_h, β_h) and plotted each as a function of voltage. They then found a fit to each rate coefficient that matched their experimental data. The final model of the sodium current is given by the following set of equations:

$$I_{Na} = \overline{g}_{Na} m^3\, h(V - E_{Na}),$$

$$\frac{dm}{dt} = \alpha_m(1-m) - \beta_m m, \qquad \frac{dh}{dt} = \alpha_h(1-h) - \beta_h h,$$

$$\alpha_m = 0.1\,\frac{V+40}{1-\exp(-(V+40)/10)}, \qquad \alpha_h = 0.07\,\exp(-(V+65)/20),$$

$$\beta_m = 4\,\exp(-(V+65)/18), \qquad \beta_h = \frac{1}{\exp(-(V+35)/10)+1}. \tag{3.18}$$

3.2.3 The leak current

Hodgkin and Huxley's evidence suggested that while potassium is a major part of the non-sodium ionic current, other ions besides sodium might carry current across the membrane. At the potassium equilibrium potential, they found that some non-sodium current still flows. This current could not be due to potassium ions since the driving force $V - E_K$ was zero. Hodgkin and Huxley proposed that it was due to a mixture of ions, and they dubbed it the leak current I_L. They assumed this was a resting background current that was not dependent on voltage. Using a quasi-ohmic current–voltage relationship they derived E_L and $\overline{g}_L$ from their experimental results. Both the leakage conductance and equilibrium potential are due largely to the permeability

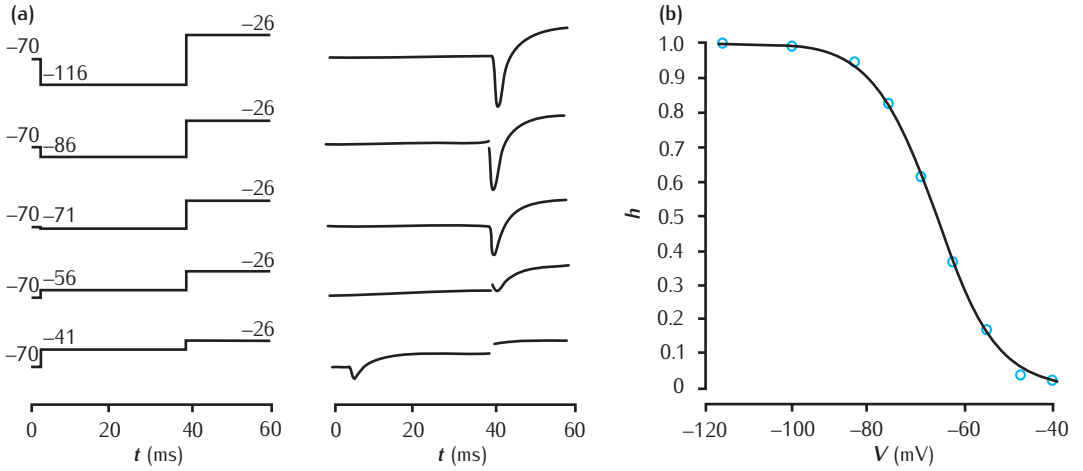

Fig. 3.8 **(a)** Two-pulse protocol used to calculate the influence of membrane potential on the inactivation of sodium in the squid giant axon. From a rest holding potential, the membrane is shifted to a test potential and then stepped to a fixed potential (−26 mV). The sodium current recorded in response to the final step (right) is influenced by the level of inactivation resulting from the test potential. **(b)** The level of inactivation as a function of the test potential (recorded current relative to the maximum current). Adapted from Hodgkin and Huxley (1952c), with permission from John Wiley & Sons Ltd.

of the membrane to chloride ions. The leak current is modelled by:

$$I_L = \overline{g}_L(V - E_L). \tag{3.19}$$

Although the leak conductance $\overline{g}_L$ in the Hodgkin–Huxley circuit and the membrane resistance R_m in the passive circuit (Chapter 2) appear similar, they have different meanings. In the HH model, the resting membrane potential differs from the electromotive force of the leak battery and the resting membrane resistance is not equal to the inverse of the leak conductance. Instead, the resting membrane potential and the resting membrane resistance are determined by the sodium, potassium and leak resting conductances. We return to this difference in Section 4.4.

3.2.4 The complete model

In the final paper of the series, Hodgkin and Huxley (1952d) inserted their expressions for the three ionic currents (Equations 3.3–3.5) into the membrane equation (Equation 3.1) to give a description of how the membrane potential in a small region of squid giant axon changes over time:

$$C_m \frac{dV}{dt} = -\overline{g}_L(V - E_L) - \overline{g}_{Na} m^3 h(V - E_{Na}) - \overline{g}_K n^4 (V - E_K) + I, \tag{3.20}$$

where I is the **local circuit current**, the net contribution of the axial current from neighbouring regions of the axon. In a continuous cable model of the axon, this contribution is the second derivative of the membrane potential with respect to space (Equation 2.24). When Equation 3.20 is put together with the differential equations for the gating variables n, m and h and the expressions for the rate coefficients (Equations 3.14 and 3.18), the resulting set of four differential equations forms the HH model. It is summarised in Box 3.5.

Equation 3.20 could equally well relate to a compartment in a compartmental model, as described in Section 2.8. In this case, the local circuit current depends on the membrane potential in the neighbouring compartments (Equations 2.20).

The system can be simplified by imposing the space clamp condition (Box 3.1) so that the membrane potential is constant over the membrane.